

Boson bound states in the β -Fermi–Pasta–Ulam model

XIN-GUANG HU¹, JU XIANG^{2,*}, ZHENG JIAO¹, YANG LIU³,
GUO-QIU XIE¹ and KE HU³

¹Department of Physics, Huangshan University, Huangshan 245041, Anhui, China

²Department of Basic Sciences, The First Aeronautical Institute of the Air Force, Xinyang 464000, Henan, China

³Department of Physics, Xiangtan University, Xiangtan 411105, Hunan, China

*Corresponding author. E-mail: xiang.ju@foxmail.com

MS received 6 March 2013; revised 12 July 2013; accepted 26 July 2013

DOI: 10.1007/s12043-013-0610-8; ePublication: 22 October 2013

Abstract. The bound states of four bosons in the quantum β -Fermi–Pasta–Ulam model are investigated and some interesting results are presented using the number conserving approximation combined with the number state method. We find that the relative magnitude of anharmonic coefficient has a significant effect on forming localized energy in the model, and the wave number plays an important role in forming different bound states. The signature of the quantum breather is also set up by the square of the amplitudes of the corresponding eigenvectors in real space.

Keywords. Discrete breather; Fermi–Pasta–Ulam model; number state method; boson bound state.

PACS Nos 63.20.Pw; 63.20.Ry; 63.20.D–

1. Introduction

Discrete breathers (DBs) or intrinsic localized modes (ILMs) which are spatially localized, time-periodic and stable (or at least long-lived) excitations have been the subject of intense theoretical researches in the past decades [1–3], and have been observed in a variety of physical systems, including one-dimensional diatomic granular crystals [4], Josephson junction arrays [5], micromechanical systems [6], and so on. In many cases, quantum dynamics plays a significant role. So a natural question arises: what remains of discrete breathers if the corresponding quantum problem is considered? To answer this question, and also for the purpose of studying quantum dots and quantum computing, many theoretical and experimental studies have been devoted to different quantum nonlinear lattices recently [7–14]. The results confirmed the existence of bound states, some of which featured a particle-like energy band, and it is now pointed out to be the natural equivalents of DB solutions of classical nonlinear systems [9]. By path integral

methods and numerical diagonalization, Schulman studied the stability of such localized states, and pointed out that the quantized discrete breather in a 1D lattice is stable [15,16]. Furthermore, the two-vibron bound states (TVBS, also known as biphonons or two-quantum bound states etc.), which have been well studied in the Klein–Gordon (KG) lattice [10,11,17] and Bose–Hubbard (BH) model [7,8,14], show that such specific excitations may be the simplest quantum equivalents of breather solutions in classical systems. In a series of recent papers, such quantum excitations have already been found in the β -Fermi–Pasta–Ulam (FPU) model [12,18], in an extended Hubbard chain [14], in α -helices [19,20], as well as in a finite Heisenberg spin chain [21]. Experimentally, the formation of TVBS is observed in molecular adsorbates such as H/Si (1 1 1) [22,23], H/C (1 1 1) [24] and so on.

It is well known that classical DBs possess rich dynamic behaviour properties. For example, in systems with both nonlinearities and impurities or defects, the existence of impurities or defects will affect the DBs (if they exist) considerably [25], and even if only nonlinearity is retained, the interaction between DBs is still interesting. Unfortunately, such studies are less in quantum system. As the first quantum states derived from nonlinearity, TVBS is the natural choice for studying such dynamic behaviour properties. Some useful results are presented in [26,27] on the interaction between impurities or defects with TVBS, some of which are similar to their classical equivalents, and the results also confirmed that the TVBS is the simplest quantum breather (QB). At the same time, other researchers published their results about the quantum signatures of breather–breather interaction in quantum nonlinear lattices [21,28], it is the TVBS interaction with each other. In fact, to explore the dynamic behaviour of quantum breathers, it is convenient to study the four boson bound states appeared in nonlinear systems, and such studies are less known. In previous studies, the degenerate perturbation theory was applied when only on-site nonlinearity was taken at weak coupling [28], but in more complicated nonlinear interaction systems (for instance, the β -FPU model), it is invalid. In the present paper, we report our results on boson bound states (BBS) in the β -FPU model. The paper is organized as follows. In §2, we first describe the model and introduce the quantization scheme, then, at 4-quanta level, we introduce the basis we used to diagonalize the effective Hamiltonian. The energy spectrum of the model at 4-quanta level and the corresponding bound states are studied in §3. Section 4 gives the conclusion of our results.

2. Model and method

The classical β -FPU model describes the nearest-neighbour interactions for a one-dimensional chain. Its Hamiltonian can be written as

$$H = \sum_n \frac{p_n^2}{2m} + \frac{k_2}{2} (x_n - x_{n-1})^2 + \frac{k_4}{4} (x_n - x_{n-1})^4, \quad (1)$$

where m is the mass of an atom, k_2 and k_4 are the nearest-neighbour harmonic and anharmonic force constants, respectively. It is known that this model can support DBs or ILMs

[29]. In order to investigate the boson bound states, we write the momentum and position operators of the n th atom as

$$\begin{aligned} p_n &= i\sqrt{\frac{\hbar m\omega}{2}}(a_n^+ - a_n), \\ x_n &= \sqrt{\frac{\hbar}{2m\omega}}(a_n^+ + a_n). \end{aligned} \quad (2)$$

Here $\omega = \sqrt{2k_2/m}$, a_n^+ and a_n are boson creation and annihilation operators, which satisfy the canonical commutation relations: $[a_m, a_n^+] = \delta_{m,n}$, $[a_m, a_n] = 0$ and $[a_m^+, a_n^+] = 0$. $\lambda = \hbar k_4/(k_2 m \omega)$ is introduced as a dimensionless parameter representing relative magnitude of anharmonic coefficient. Within the number conserving approximation and periodic boundary condition, the effective Hamiltonian of the β -FPU model can be obtained as

$$\begin{aligned} \hat{H}_{\text{eff}} &= \hbar\omega \left\{ \frac{N}{2} \left(1 + \frac{3}{4}\lambda \right) + \left(1 + \frac{3}{2}\lambda \right) \sum_n a_n^+ a_n \right. \\ &\quad - \frac{1}{4} (1 + 3\lambda) \sum_n a_n^+ (a_{n+1} + a_{n-1}) \\ &\quad + \frac{3}{8}\lambda \sum_n \left[a_n^+ a_n^+ a_n a_n + \frac{1}{2} a_n^+ a_n^+ (a_{n+1} a_{n+1} + a_{n-1} a_{n-1}) \right] \\ &\quad + \frac{3}{8}\lambda \sum_n \left[a_n^+ a_n (a_{n+1}^+ a_{n+1} + a_{n-1}^+ a_{n-1}) \right. \\ &\quad \left. \left. - (a_n^+ a_n^+ a_n a_{n+1} + a_n^+ a_n^+ a_n a_{n-1} + \text{h.c.}) \right] \right\}, \end{aligned} \quad (3)$$

where N is the total number of atoms. It is worth noting that the same procedure was adopted in refs [12,30] in the same model, and ref. [30] gave a more detailed description of it. More recently, Riseborough [31] reported his results about the quantized breather excitations by employing many-body theory and keeping the non-conserving terms in the same model, and his conclusion is in agreement with the results given by the number conserving approximation methods for monoatomic β -FPU lattice at $n = 2$ level [12,18], and ref. [32] constructed quantum solutions of β -FPU model based on enumerating simple periodic orbits; the results are very interesting for understanding the concept of phonon in the nonlinear system; it may be used for understanding the properties of QBs.

Note that eq. (3) conserves the total number of bosons, and so it is more convenient to employ number state method (NSM) to proceed with our analysis in the model. The NSM has been widely used to study the TVBS [7,8,13,18,21,26,28]. The number operator is

$$\hat{N}_1 = \sum_{j=1}^N a_j^+ a_j, \quad (4)$$

which has eigenvalue n . Under the periodic boundary conditions, Hamiltonians (3) is invariant under the action of the translation operator \hat{T} with eigenvalue $\exp(i \cdot k \cdot a)$, where

$k = 2\pi v/(N \cdot a)$, a is the lattice constant and v is an integer. \hat{T} is defined by the property $\hat{T}a_j^+ = a_{j+1}^+\hat{T}$ so that $\hat{T}[n_1n_2 \cdots n_N] = [n_Nn_1 \cdots n_{N-1}]$, n_i denotes the quanta at the site i and $\sum_{i=1}^N n_i = n$. To describe the components of the quantum states, we use a position state basis representation. For example, the state $|\varphi_j\rangle = |2010010 \cdots 0\rangle$ represents a state with two bosons at site 1, one boson at site 3, one boson at site 6 and no bosons elsewhere. In view of the periodic structure of the lattice, and the translationally invariant nature of the chain, the effective Hamiltonian of this quantum system commutes with the number operator $\hat{N}_1 = \sum_{j=1}^N a_j^+ a_j$, whose eigenvalue is denoted by n as mentioned above. We can generate an equivalence class of states by applying the translation operator with periodic boundary conditions to one of these states, for example, $|201010 \cdots 0\rangle$ and $|0201010 \cdots 0\rangle$ are the equivalence class states. We can manage to order these classes. For instance, the set of all classes containing $|211\rangle$, $|20101\rangle$, $|20 \cdots 010 \cdots 10 \cdots 0\rangle$, and so on, is referred to as the $\{2,1,1\}$ band. All classes containing $|220 \cdots 0\rangle$, $|2020 \cdots 0\rangle$, \dots are referred to as the $\{2,2\}$ band. For $n = 4$, the total bands are five, that is, $\{4\}$, $\{3,1\}$, $\{2,2\}$, $\{2,1,1\}$ and $\{1,1,1,1\}$. For simplicity, we consider $N = 11$, and in this case, it is easy to counter the number of all number states: $\{4\}$ band contains only one equivalence class state, and the band of $\{3,1\}$ contains 10, $\{2,2\}$ contains 5, $\{2,1,1\}$ contains 45, $\{1,1,1,1\}$ contains 30, and the sum is 91 equivalence class states. For $n = 4$ and $N = 19$, the total number of equivalence class states is 384. We use $|\Psi\rangle$ as a general eigenstate of eq. (3),

$$|\Psi\rangle = \sum_{j=1}^{91} C_j |\psi_j\rangle \tag{5}$$

which requires that $\hat{H}_{\text{eff}}|\Psi\rangle = E|\Psi\rangle$ leading to the matrix equation

$$H_{\text{eff}}(k)c = Ec, \tag{6}$$

where $H_{\text{eff}}(k)$ is 91×91 matrix and $c = \text{col}(c_1, c_2, \dots, c_{91})$. We can calculate the eigenvalues and the corresponding eigenvectors exactly by the standard method from a numerical library [33].

3. Energy spectrum and boson bound states

In figures 1, 2 and 3 we show the energy spectrum of the effective Hamiltonian matrix (3) obtained by numerical diagonalization for different parameters of relative magnitude of anharmonic coefficient λ at 4 quanta level and 11 sites. At $\lambda = 0$, the spectrum is composed of quasicontinuum band, whose eigenstates are characterized by the four bosons independently moving along the lattice. The same quasicontinuum band is also observed in figures 1, 2 and 3 for nonzero nonlinear interaction. However, in addition to the continuum, one or two discrete bands dropped out of the quasicontinuum band are observed, depending on the parameter λ and the wave number q (see figures 1b–1d, 2b–2d and 3a and 3b). The phenomenon that two discrete bands appear for some proper negative λ but only one exists when λ is positive (actually speaking, an isolated eigenvalue appeared between the continuum band and the first discrete band at the edge of the first

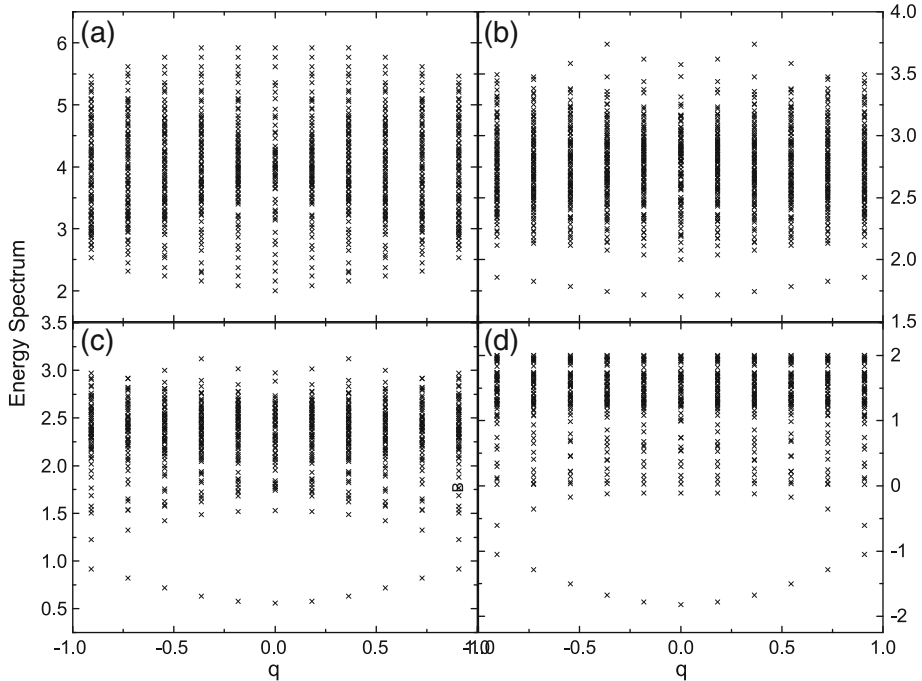


Figure 1. Energy spectrum of $H_{\text{eff}}(k)$. The eigenvalues are plotted as a function of the wave number q for different values of λ : (a) $\lambda = 0$, (b) $\lambda = -1/6$, (c) $\lambda = -2/9$, (d) $\lambda = -1/3$. The chain is composed of $N = 11$ sites. The y-axis is measured in units of $\hbar\omega$ while x-axis bears the dimensionless $q = k \cdot a/\pi$ in the first Brillouin zone. The term $(N/2)(1 + (3/4)\lambda)$ in eq. (3) does not contribute to the spectrum, and so it is not considered in the energy spectrum.

Brillouin zone, see figure 3b) means that the relative magnitude of anharmonic coefficient has a significant effect on forming localized energy in the model. To explore the properties of the dropped one or two discrete bands, we investigate the energy spectrum for other values of λ , as shown figure 2. A discrete band starts dropping out of the continuum when λ is about -0.16 for all values of q , as can be seen in figures 1b and 2a. If $|\lambda|$ increases at negative direction, to about -0.2 , the second discrete band begins to appear in the energy spectrum at the edge of the first Brillouin zone (BZ) (see figure 2b), and when λ decreases to $-2/9$, the whole second discrete band is completely separated from the continuum spectrum almost at all the BZ (see figure 1c); however, with decreasing λ , the second discrete band progressively merges into the continuum band at the centre of the BZ (see figures 1d and 2c). If the attractive nonlinearity ($\lambda < 0$) is strong enough, only the edge of the second discrete band remains (see figure 2d). Figure 3 exhibits the results of positive values of λ . One discrete eigenvalue out of the continuum band and the discrete band can still be seen in figure 3b at the edge of BZ, it is similar to the case of the strong attractive nonlinearity. We note that the appearance of the second discrete band has already been observed in ref. [14] at 2 quanta level for strong intersite nonlinear interaction.

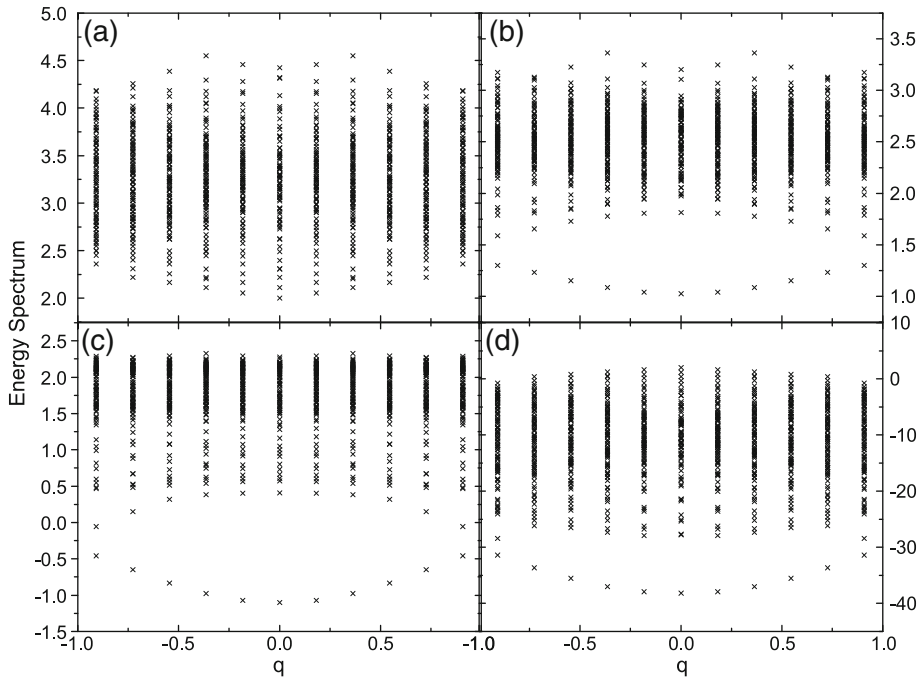


Figure 2. Energy spectrum of $H_{\text{eff}}(k)$. The eigenvalues are plotted as a function of the wave number q for other values of λ : (a) $\lambda = -0.1$, (b) $\lambda = -0.2$, (c) $\lambda = -0.3$, (d) $\lambda = -2$.

To investigate the probability of a given localized state for the corresponding β -FPU chain, we also plotted the square of the eigenvectors in real space for different values of λ in figures 4 and 5. The examination of the corresponding eigenvectors of the discrete band shows that different bound states exist in the model. In the continuum band most of the

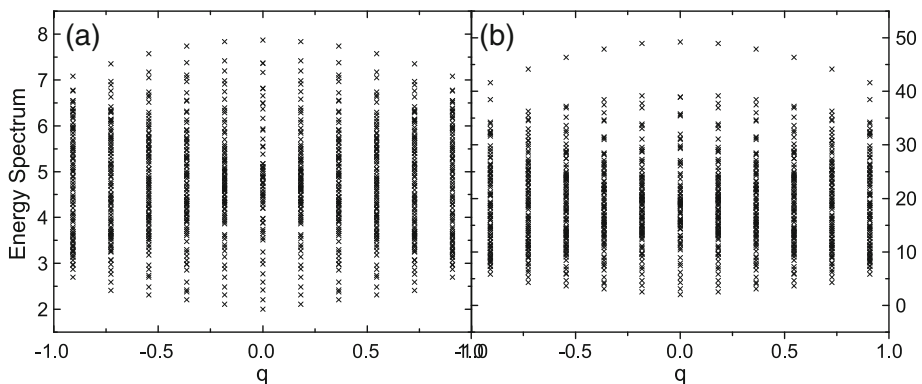


Figure 3. Energy spectrum of $H_{\text{eff}}(k)$, for repulsive nonlinearity: (a) $\lambda = 0.1$, (b) $\lambda = 2$.

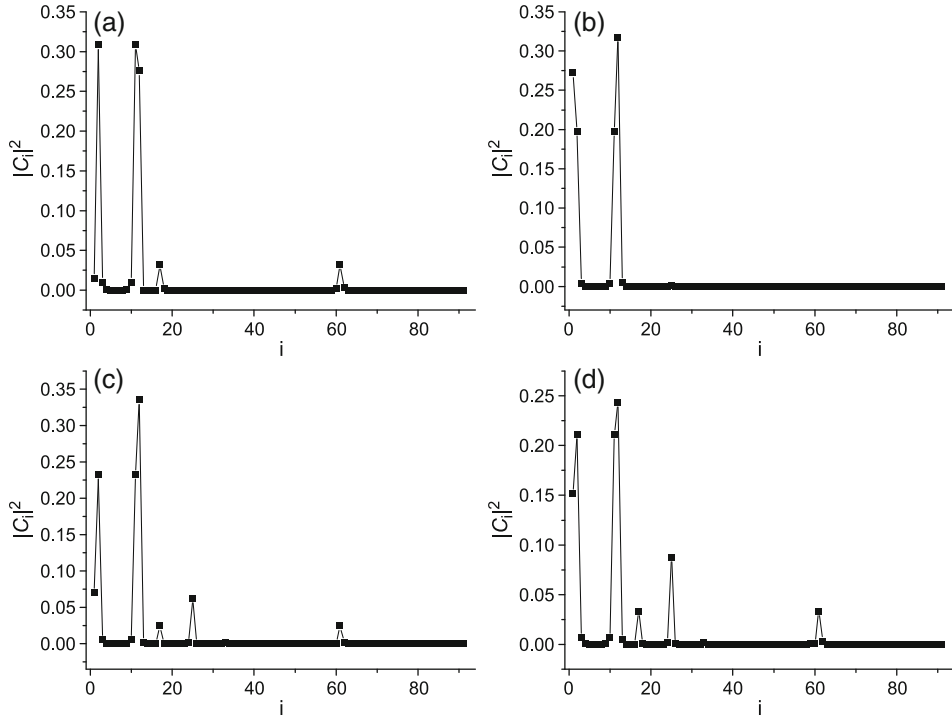


Figure 4. Boson bound states corresponding to the first discrete band for (a) $\lambda = -1/6$, $q = -10/11$, (b) $\lambda = -1/6$, $q = 0$, (c) $\lambda = -2$, $q = -10/11$, (d) $\lambda = -2$, $q = 0$.

sites are separated by one or more vacant sites, and we do not consider these bands. The three high points in figure 4a show that there is a high probability of finding three bosons on one site and one boson on the adjacent site at the same time ($|310 \dots 0\rangle$, $|30 \dots 01\rangle$) equivalent class bound states, we call it 3-1 bosons bound states) as well as two bosons on one site and another two on the adjacent site ($|220 \dots 0\rangle$) equivalent class bound states, 2-2 bosons bound states) simultaneously. Figure 4b presents the case when wave number $q = 0$ (i.e. wave number approaches the central BZ), four high points appeared in the figure, which represent the high probability of finding four bosons on the same site (4 bosons bound states), 2-2 bound states and 3-1 bosons bound states respectively. However, compared to the edge of the BZ, for example, figure 4a, the probability of finding 2-2 bound states is higher than 3-1 bound states. If the nonlinearity becomes strong enough, all the three bound states mentioned above can survive in the model, and 2-2 bound states will dominate the system compared to 3-1 and 4 bound states (see figures 4c and 4d).

The second discrete band appearing in the energy spectrum also attracts our attention. Physically speaking, they are the localized energy too, and we can see from figure 1 that the energy of such cases lies between the first discrete band the continuum band. The probability function of the bound states corresponding to the second discrete band is plotted in figure 5. Figure 5a shows that apart from 4 and 3-1 bound states, there is a high

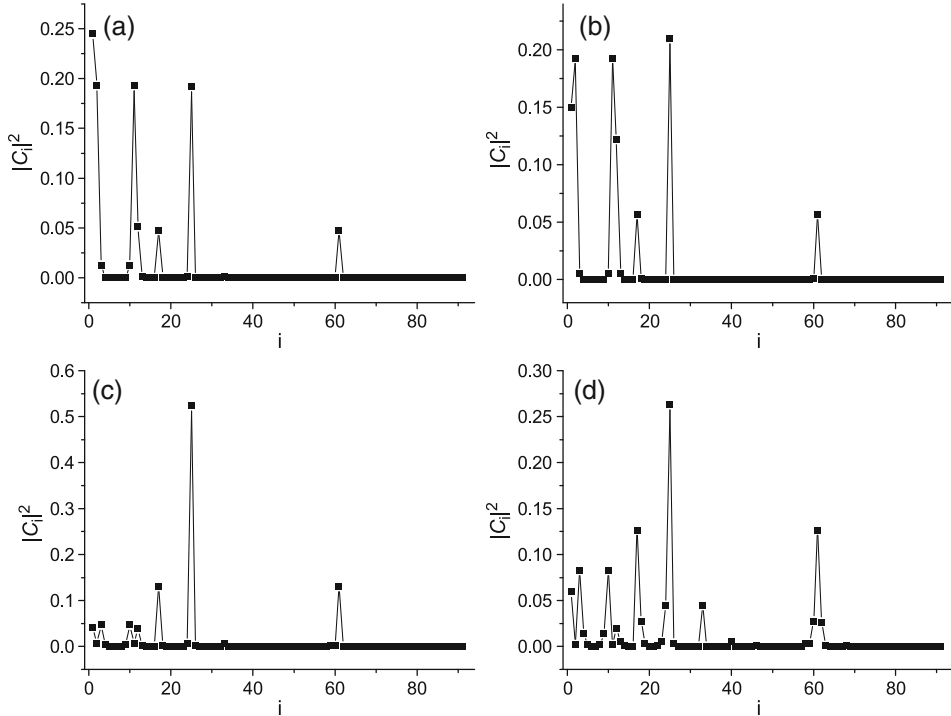


Figure 5. Boson bound states corresponding to the second discrete band for (a) $\lambda = -1/3$, $q = -10/11$, (b) $\lambda = -2$, $q = -10/11$, (c) $\lambda = -2/9$, $q = 0$, (d) $\lambda = -1/3$, $q = 0$. Actually speaking, just one isolated energy dot located between the quasicontinuum band and the first discrete band (see figure 2d).

probability of finding two bosons on the same site while the other two bosons are on both sides of the two-boson site (1-2-1 bound states), if λ approaches -2 and also at the edge of the BZ, the 3-1 bound states remain and the probability of finding the 4 bound states decreases while 1-2-1 bound states increases, and 2-2 bound states cannot be ignored (see figure 5b). Figure 5c shows the result at the centre of the BZ. In this case, only 1-2-1 bound states survive while other bound states almost disappear, and with nonlinearity increasing, the centre of the second band gradually merges with the continuum band, and so the bound states approach to disappear (see figure 5d), that is, most of the sites are separated by one or more vacant sites. We have not plotted the graph of $|C_i|^2$ vs. i when $\lambda > 0$ because the bound states are similar to what we have obtained for $\lambda = -2$.

For understanding the fine structure of the energy spectrum as well as its corresponding bound states, we have investigated the matrix elements of eq. (6). When $\lambda = -1/3$, we found that most of the elements $H_{m,m+1}$ are zero, where m is a variable ranging from 1 to 90, which means that the interaction between the two neighbouring states we arranged is very weak which will help the system to form localized energy, as plotted in figure 1d. When $\lambda = -2/9$, the element which links the $\{2,2\}$ state and the $\{2,1,1\}$ state is 0. However, the interaction between two neighbouring states is non-zero, and so the bound

states in this case are in the form of 1-2-1 bound states (see figure 5c). When $\lambda = -1/6$, the element which also links the $\{2,2\}$ state and the $\{2,1,1\}$ state is 0, but the relative magnitude of anharmonic coefficient is so weak that the second discrete band cannot be formed in the system. We did not discuss the case of the other values of λ because they do not own such properties.

In strong on-site nonlinear and weak coupling systems, such as Bose–Hubbard model [28], one has obtained the quantum signatures of breather–breather interactions by using degenerate perturbation method: the state $|220 \dots 0\rangle$ splits from the rest of the band ($|2020 \dots 0\rangle$, $|20020 \dots 0\rangle$, etc.), which means that there is a high probability of finding two bosons on the same site while the other two on the adjacent site. However, in more complex systems, for example, in systems of intersite nonlinear interactions, the energy spectrum of $\{2,2\}$ is not degenerated, and the degenerate perturbation method is invalid; furthermore, in this case, there is a competition between the coupling term and the intersite nonlinear interaction term, which will make the bound states more complicated, as discussed above.

From figures 4, 5a and 5d, we can also find that the wave number has a significant impact on the formation of different bound states. Similar results are also reported in ref. [14].

4. Conclusions

We quantized the β -FPU model within the boson quantization rules combined with the number conserving approximation. Then, by using the NSM, the energy spectrum of the quantized β -FPU model at four-quanta level was obtained. Our results confirmed that when the nonlinearity is significant, one or two discrete bands will separate from the quasicontinuum band. It is similar to the energy spectrum at two-quanta level in other nonlinear models [14], but exhibits more dynamic behaviour. We gave a description of the signature of the quantum breathers by the square of the amplitudes of the corresponding eigenvectors in real space, several bound states are found. We also found that the wave number plays a significant role in forming different bound states. Finally, we gave a qualitative analysis of the fine structure of the energy spectrum as well as its corresponding bound states. We also presented the difference between our results and other results.

Acknowledgement

The authors would like to thank Dr Li Shihua and Zhang Jun for interesting comments and suggestions. The work has been supported by the scientific research project of Huangshan University under Grant No. 2011xkj007 and the Project of Anhui Provincial Educational Department of China under Grant No. KJ2011Z363.

References

- [1] S Flach and A V Gorbach, *Phys. Rep.* **467**, 1 (2008)
- [2] P Maniatis, B S Alexandrov, A R Bishop and K Ø Rasmussen, *Phys. Rev. E* **83**, 011904 (2011)

- [3] H Hennig, J Dornignac and D K Campbell, *Phys. Rev. A* **82**, 053604 (2010)
- [4] N Boechler, G Theocharis, S Job, P G Kevrekidis, M A Porter and C Daraio, *Phys. Rev. Lett.* **104**, 244302 (2010)
- [5] E Trías, J J Mazo and T P Orlando, *Phys. Rev. Lett.* **84**, 741 (2000)
- [6] M Sato, B E Hubbard, A J Sievers, B Ilic, D A Czaplewski and H G Craighead, *Phys. Rev. Lett.* **90**, 044102 (2003)
- [7] J C Eilbeck, H Gilhøj and A C Scott, *Phys. Lett. A* **172**, 229 (1993)
- [8] A C Scott, J C Eilbeck and H Gilhøj, *Physica D: Nonlinear Phenomena* **78**, 194 (1994)
- [9] W Z Wang, J T Gammel, A R Bishop and M I Salkola, *Phys. Rev. Lett.* **76**, 3598 (1996)
- [10] L Proville, *Physica D: Nonlinear Phenomena* **216**, 191 (2006)
- [11] L Proville, *Phys. Rev. B* **71**, 104306 (2005)
- [12] Z Ivić and G P Tsironis, *Physica D: Nonlinear Phenomena* **216**, 200 (2006)
- [13] J P Nguenang, R A Pinto and S Flach, *Phys. Rev. B* **75**, 214303 (2007)
- [14] J P Nguenang and S Flach, *Phys. Rev. A* **80**, 015601 (2009)
- [15] L S Schulman, D Tolkunov and E Mihóková, *Chem. Phys.* **322**, 55 (2006)
- [16] L S Schulman, D Tolkunov and E Mihokova, *Phys. Rev. Lett.* **96**, 065501 (2006)
- [17] L Proville, *Europhys. Lett.* **69**, 763 (2005)
- [18] H Xin-Guang and T Yi, *Chin. Phys. B* **17**, 4268 (2008)
- [19] V Pouthier, *Phys. Rev. E* **68**, 021909 (2003)
- [20] C Falvo and V Pouthier, *J. Chem. Phys.* **123**, 184710 (2005)
- [21] Z I Djoufack, A Kenfack-Jiotsa, J P Nguenang and S Domngang, *J. Phys.: Condens. Matter* **22**, 205502 (2010)
- [22] R Honke, P Jakob, Y J Chabal, A Dvořák, S Tausendpfund, W Stigler, P Pavone, A P Mayer and U Schröder, *Phys. Rev. B* **59**, 10996 (1999)
- [23] P Guyot-Sionnest, *Phys. Rev. Lett.* **67**, 2323 (1991)
- [24] R P Chin, X Blase, Y R Shen and S G Louie, *Europhys. Lett.* **30**, 399 (1995)
- [25] G Theocharis, N Boechler, P G Kevrekidis, S Job, M A Porter and C Daraio, *Phys. Rev. E* **82**, 056604 (2010)
- [26] V Pouthier, *Phys. Rev. B* **71**, 115401 (2005)
- [27] J C Eilbeck and F Palmero, *Phys. Lett. A* **331**, 201 (2004)
- [28] J Dornignac, J C Eilbeck, M Salerno and A C Scott, *Phys. Rev. Lett.* **93**, 025504 (2004)
- [29] A J Sievers and S Takeno, *Phys. Rev. Lett.* **61**, 970 (1988)
- [30] Z-P Shi and G Huang, *Phys. Rev. B* **44**, 12601 (1991)
- [31] P S Riseborough, *Phys. Rev. E* **85**, 011129 (2012)
- [32] R L Sonone and S R Jain, *Eur. Phys. J. Special Topics* **222**, 601 (2013)
- [33] W H Press, S A Teukolsky, W T Vetterling and B P Flannery, *Numerical recipes in FORTRAN* (Cambridge University Press, 1992) pp. 462–475